Supplementary Information for:

Green and scalable production of colloidal perovskite nanocrystals and transparent sols by controlled self-collection process

Shuangyi Liu, Limin Huang, Wanlu Li, Xiaohua Liu, Jing Shui, Jackie Li, and Stephen O'Brien

Contents

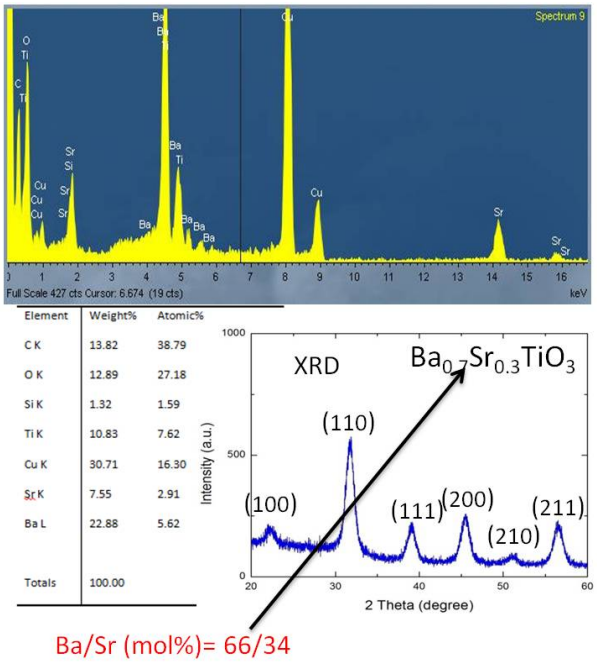

Figure S1. XRD and elemental analysis of BST nanocrystals by HRSEM equipped with an EDX system.

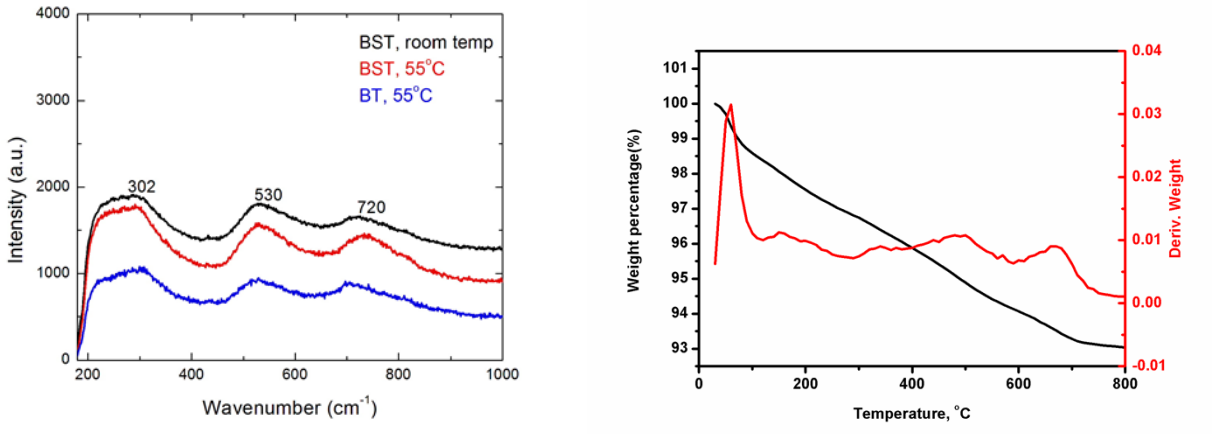

Figure S2. Right: Room temperature Raman spectra of BT/BST nanocrystals synthesized at different temperatures. Left: TGA/DTG profile of 8 nm BST nanoparticles in flowing N_2(g), for comparison with TGA/DTG profile in air (manuscript Figure 4).

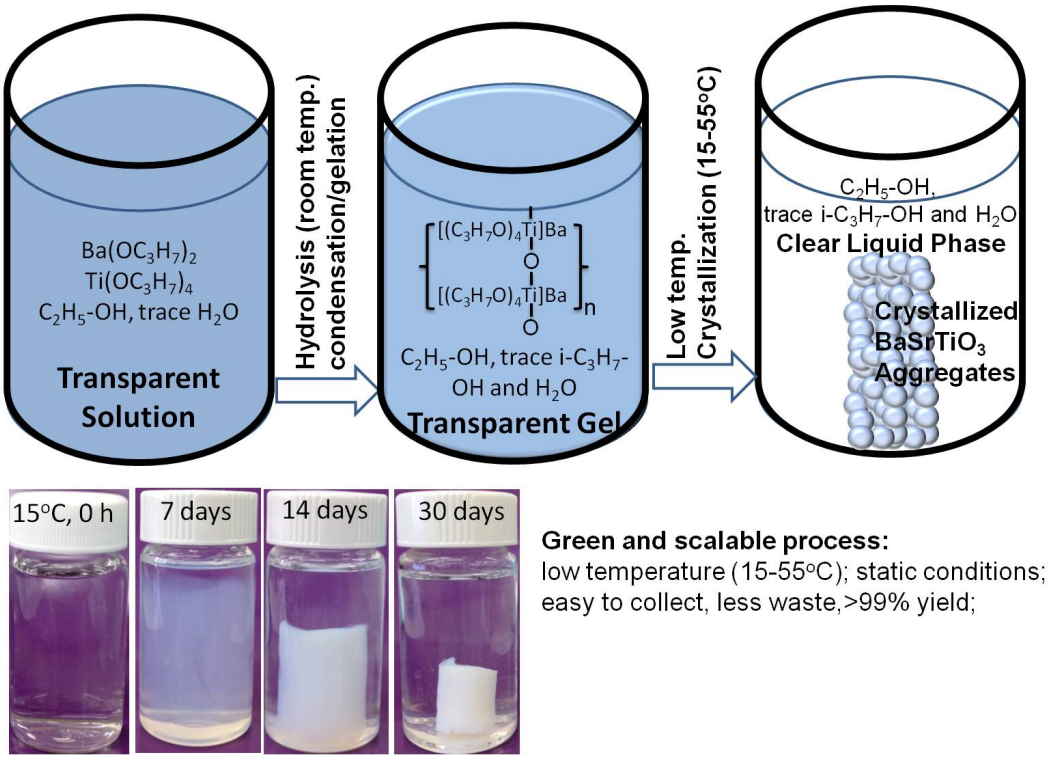

Figure S3. Graphic abstract of reaction process.

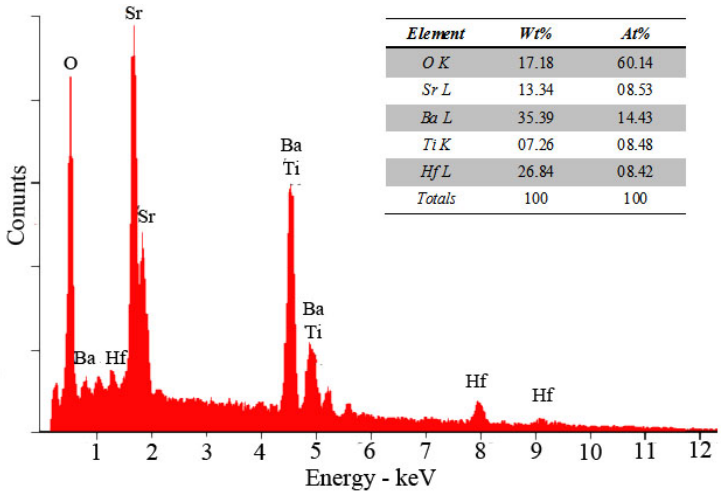

Element	Wt%	At%
O K	17.18	60.14
Sr L	13.34	08.53
Ba L	35.39	14.43
Ti K	07.26	08.48
Hf L	26.84	08.42
Totals	100	100

Figure S4 EDX spectrum of as-synthesized BSTH nanocrystals.

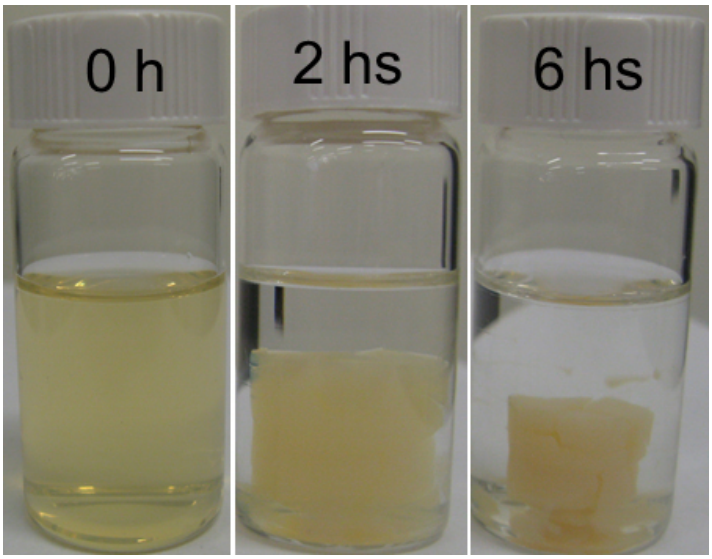

Figure S5. BST nanocrystals synthesis using $Sr(OiPr)_2$ as a metalorganic source (55°C).

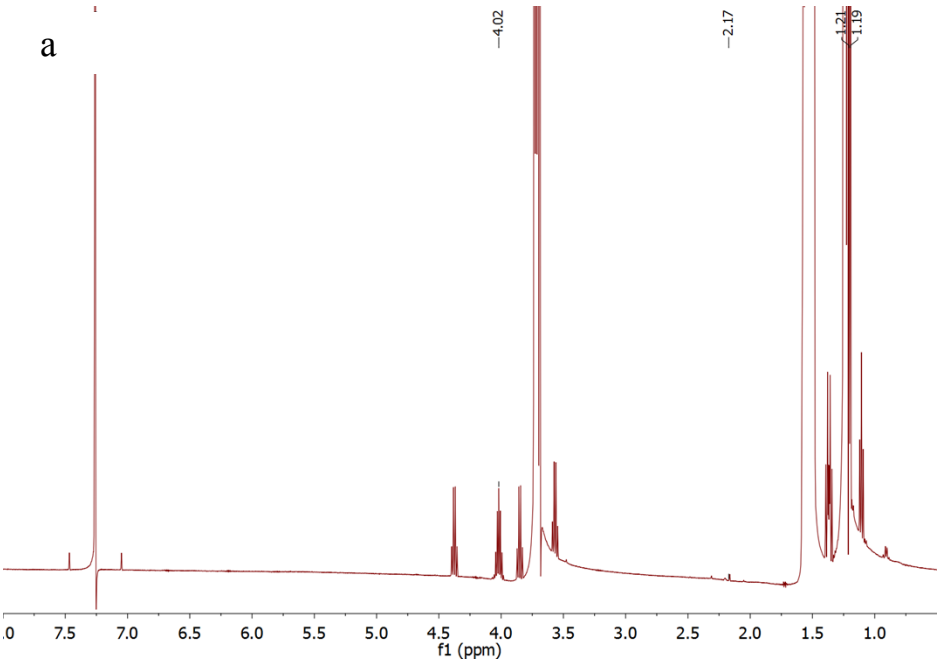

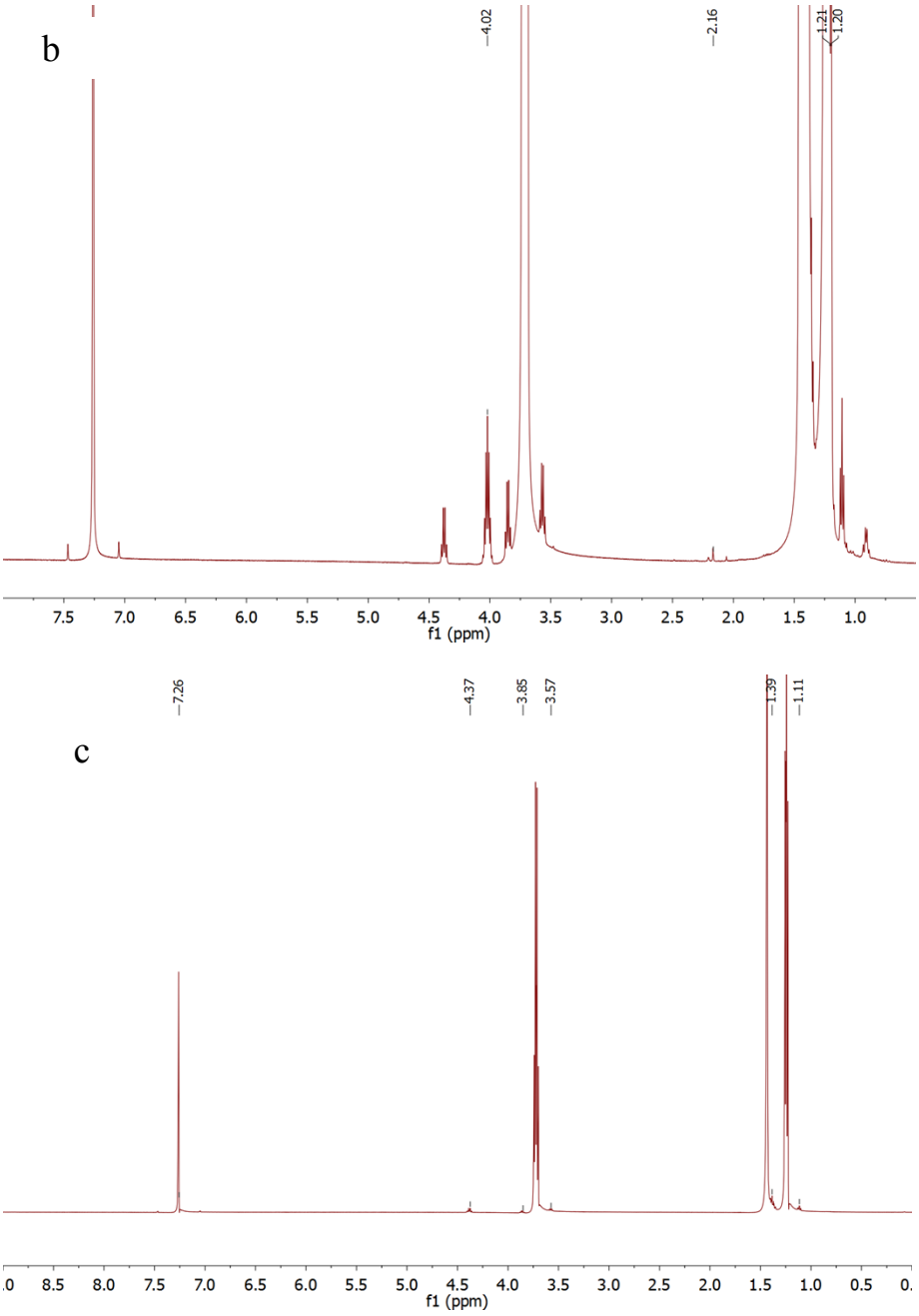

Figure S6. (a) ^{1}H NMR spectrum of the BST mother solution after reaction. The most intense peaks come from the solvent ethanol. The reference spectra of ethanol from SDBS is ^{1}H NMR (CDCl3, 25℃, ppm): δ=1.226 (t,3H), 2.61 (s, 1H), 3.687 (m, 2H). 2-isopropanol arising from hydrolysis was detected, whose peaks are labeled in the spectrum. The reference spectra of 2-isopronal according to SDBS is 'H NMR (CDCl3, 25℃, ppm): δ=1.20(d, 6H), 2.16 (s, 1H), 4.008 (m, 1H). The small peaks (δ=4.37, 3.85, 3.57, 1.39 and 1.11) in the NMR spectra are from the impurities from the solvent ethanol (as shown in the spectrum of the ethanol). The peak (δ=1.51) is from hydrogen bonding of hydroxyl proton, which is typically observed over a range

of chemical shift values. (b) the ^{1}H NMR spectrum of barium isopropoxide, strontium isopropoxide, and titanium isopropoxide dissolved in the ethanol. The most intense peaks come from the solvent ethanol. The methyl proton and methine proton of metal isopropoxides are detected whose peaks are labeled in the spectrum. The peak around 2.17 is from little amount of hydroxyl proton influenced by the metallic ions. The reference spectra of 2-isopropanol according to SDBS is 'H NMR (CDCl3, 25℃, ppm): δ=1.20(d, 6H), 2.16 (s, 1H), 4.008 (m, 1H). The small peaks (δ=4.37, 3.85, 3.57, 1.39 and 1.11) in the NMR spectra are from the impurities from the solvent ethanol. (c) ^{1}H NMR spectrum of ethanol, which proves that the small peaks (δ=4.37, 3.85, 3.57, 1.39 and 1.11) in the NMR spectra are from impurities from the solvent ethanol.

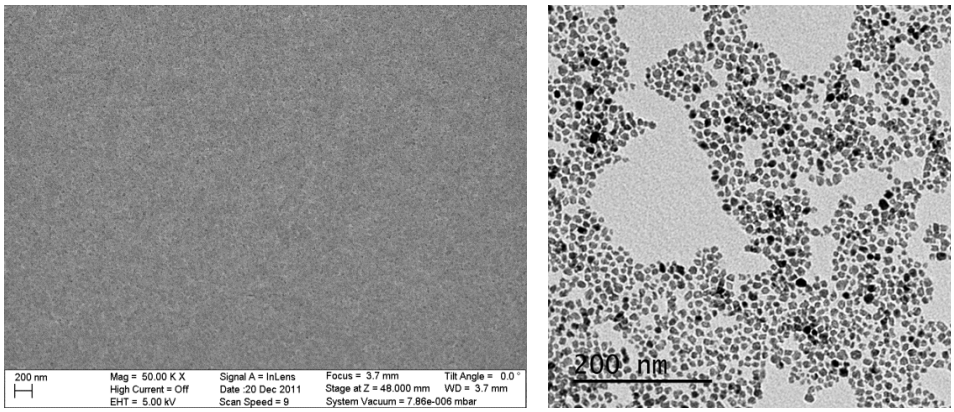

Figure S7. (left) SEM image of a BST nanocrystal thin film spin-coated with the as-synthesized stable and transparent nanocrystal solution; (right) TEM image of the as-synthesized BST nanocrystals (~7 nm).

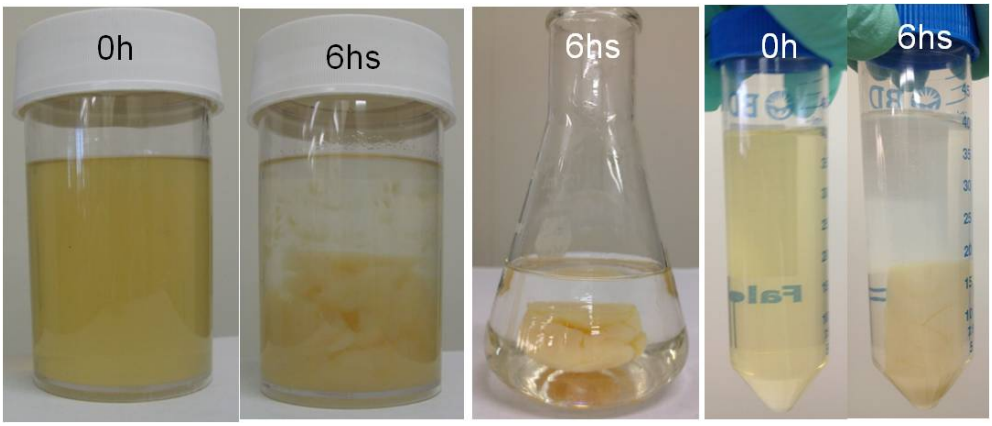

Figure S8. Low temperature synthesis of BST nanocrystals in different plastic or glass containers.

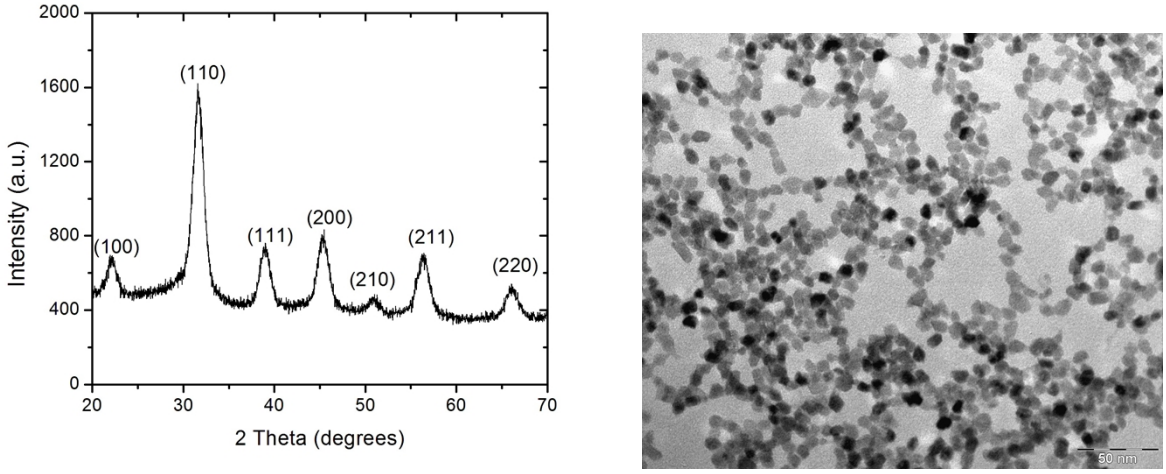

Figure S9. (left) XRD and (right) TEM image of scale-up synthesized BST nanocrystals (55^{o}C for 6 hrs).

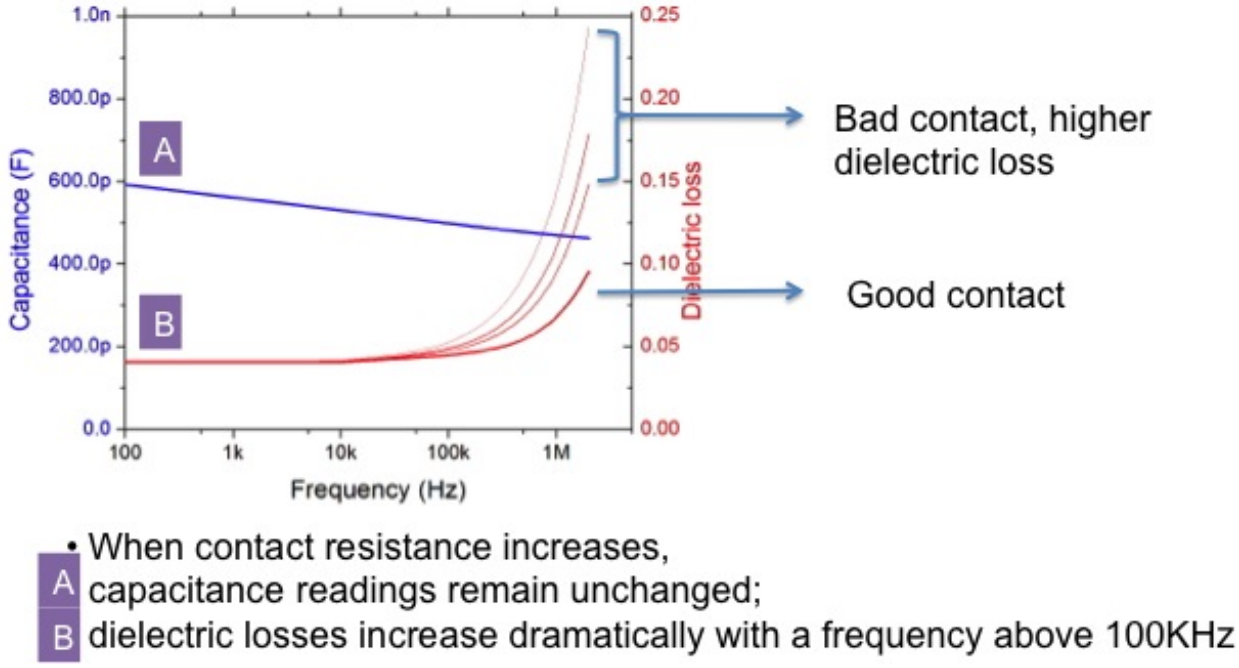

Figure S10. Contact resistance and dielectric loss. The data and text provide an explanation for how contact resistance (good vs bad contacts) affects the dielectric loss at higher frequencies during an impedance measurement. Contact resistance is an effect related to the electrode-dielectric interface, and is dependent upon choice of metal electrode (whether Al, Ag, Au, Cu etc.), quality (grain size, thickness, surface adhesion to the dielectric layer) of the metal electrodes, and the deposition process (sputtering, evaporation etc.).

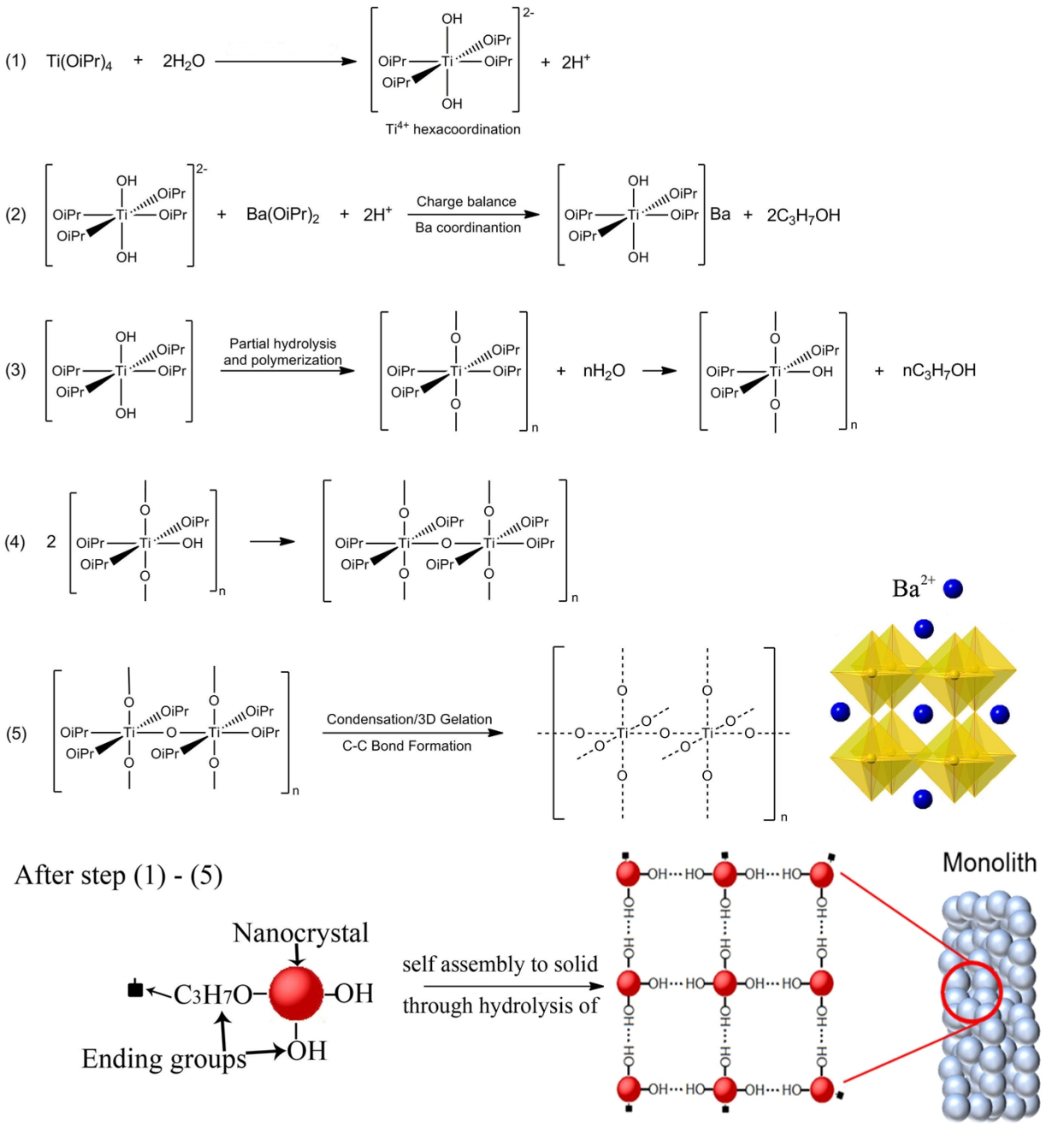

Scheme S1 Proposed growth mechanism of nanocrystals ($BaTiO_3$ as an example). After the addition of water, titanium isopropoxide first forms six-coordinated complexes with two additional OH^- ligands because such intermediate structure is popular for the d^0 transition metal cations (step 1). The occurrence of step 1 was proved by the pH values before (~7) and after (~6) addition of the water. Because OH^- ligands are easy to form through hydrolysis, fast 3D crosslink by formation of B-O-B bonds would carry out through the hydrolysis of two OH^- with each of them coming from different Ti octahedral frameworks (as shown in step 4 and 5). The degree of

3D polymerization depends on the amount of water in the solution, and the nanoparticle sizes are also decided at the step (step 3 and 4). Meanwhile, Ba^{2+} would coordinate with negative Ti six-coordinated complexes ($[Ti(OiPr)_6]^{2-}$) due to local charge balance (step 2). A Ti based chain structure (seed nuclei) was produced following the equations (1), (2) and (3). The initial transparent solution gradually becomes viscous until it totally loses liquidity due to the cross-linking of neighboring Ti based chain structures and a 3D transparent immobile gel is formed in a short time period (e.g. 30 mins for initial $[Ti(OiPr)_4]$ of 0.07 M) at room temperature under static conditions. The further slow condensation/ crystallization process, which gradually shrinks the gel and produces nanocrystal monoliths, also occurs at a low temperature of 15°C-55°C (a bit warming) under static conditions after a period of room temperature aging. The weakly bonded (hydrogen bond) nanocrystals can be easily separated and dispersed in solvent by simple sonication.

Table S1. Crystal sizes change with crystallization time

Sample (temp x time)	Crystal size (based on broadening of diffraction line (110)
BST (55 °C x 2hrs)	~6.2 nm
BST (55 °C x 3hrs)	~6.5 nm
BST (55 °C x 5hrs)	~6.6 nm

According to the Scherer equation, the crystal sizes can be estimated based on the broadening of diffraction line (110) for samples.

Table S2. Lattice parameters of samples based on the diffraction peak of (111) of cubic phase.

Sample	Lattice parameter *a* (nm)
$Ba_{0.65}Sr_{0.35}Ti_{0.5}Hf_{0.5}O_3$ (BSTH)	0.4052 nm
$BaTiO_3$ (BT)	0.4031 nm
$Ba_{0.7}Sr_{0.3}TiO_3$ (BST)	0.4005 nm
$Ba_{0.65}Sr_{0.35}TiO_3$ (BST)	0.3984 nm

These lattice parameters based on the conventional powder XRD recorded on a PANalytical X'Pert Pro Powder Diffraction instrument (or equivalent). Although the parameters (*a*) may not be fully accurate, they show a clearly defined trend with changing Ba/Sr ratios and Ti/Hf, which is consistent with the discussion in the text.